Hidden Order Transition in URu_2Si_2 and the Emergence of a Coherent Kondo Lattice

Ting Yuan, Jeremy Figgins and Dirk K. Morr
Department of Physics, University of Illinois at Chicago, Chicago, IL 60607, USA
(Dated: January 14, 2011)

Using a large-N approach, we demonstrate that the differential conductance and quasi-particle interference pattern measured in recent scanning tunneling spectroscopy experiments (A.R. Schmidt *et al.* Nature **465**, 570 (2010); P. Aynajian *et al.*, PNAS **107**, 10383 (2010)) in URu_2Si_2 are consistent with the emergence of a coherent Kondo lattice below its hidden order transition (HOT). Its formation is driven by a significant increase in the quasi-particle lifetime, which could arise from the emergence of a yet unknown order parameter at the HOT.

PACS numbers: 74.55.+v, 75.20.Hr, 71.27.+a, 72.15.Qm

Heavy-fermion materials exhibit a plethora of exciting phenomena [1] which are believed to arise from the competition between Kondo screening [2] and antiferromagnetic ordering [3]. One of the most puzzling phenomena arises in the heavy-fermion compound URu_2Si_2 which exhibits an onset of Kondo screening around $T \approx 55$K [4, 5], and undergoes a second order phase transition at $T_0 = 17.5$K [4–6] into a state with a still unknown (hidden) order parameter. Currently, an intense debate focuses on the nature of this *hidden order transition* (HOT) and its microscopic origin [5, 7]. Important new insight into this question has recently been provided by groundbreaking scanning tunneling spectroscopy (STS) experiments [8, 9]. Above the HOT, the differential conductance, dI/dV, exhibits a characteristic Fano lineshape [10]. In contrast, below T_0, a soft gap opens up in dI/dV [8, 9] and a quasi-particle interference (QPI) analysis reveals a band structure similar to that expected in the (heavy Fermi liquid) phase of a screened Kondo lattice [8]. Whether the observed changes in dI/dV below the HOT are consistent with the observed QPI pattern and with the emergence of a coherent Kondo lattice, is an important question whose answer will provide crucial insight into the nature of the hidden order transition.

In this Letter, we address this question and demonstrate that the experimentally observed dI/dV [8, 9] and QPI pattern [8] below the HOT are consistent with the emergence of a coherent Kondo lattice (CKL) and its electronic band structure. In particular, dI/dV exhibits characteristic signatures of the Kondo lattice band structure [9], such as an asymmetric gap, and a peak inside the gap which arises from the van Hove singularity of the heavy f-electron band. In addition, the temperature evolution of dI/dV [8, 9] suggests that the formation of the CKL below the HOT is primarily driven by a significant increase in the coherence, i.e., lifetime, of the heavy quasi-particles. Since the creation of a CKL is not expected to be the primary source of the observed second order phase transition at T_0, we suggest that the increased quasiparticle coherence is a result of the yet unknown order parameter that emerges at the HOT.

The starting point for our study is the Kondo-Heisenberg Hamiltonian [11–13]

$$\begin{aligned}\mathcal{H} &= \sum_{\mathbf{k},\sigma} \varepsilon_{\mathbf{k}} c^\dagger_{\mathbf{k},\sigma} c_{\mathbf{k},\sigma} + J \sum_{\mathbf{r},\alpha,\beta} \mathbf{S}^K_{\mathbf{r}} \cdot c^\dagger_{\mathbf{r},\alpha} \boldsymbol{\sigma}_{\alpha\beta} c_{\mathbf{r},\beta} \\ &\quad + \sum_{\mathbf{r},\mathbf{r}'} I_{\mathbf{r},\mathbf{r}'} \mathbf{S}^K_{\mathbf{r}} \cdot \mathbf{S}^K_{\mathbf{r}'} \; . \end{aligned} \tag{1}$$

We use a hole-like two-dimensional (2D) conduction (c-electron) band dispersion $\varepsilon_{\mathbf{k}} = 2t(\cos k_x + \cos k_y) - \mu$ with nearest-neighbor hopping t and chemical potential μ to reproduce the 2D QPI dispersion [8]. $c^\dagger_{\mathbf{k},\alpha}(c_{\mathbf{k},\alpha})$ creates (annihilates) a c-electron with spin α and momentum $\mathbf{k}$. $J > 0$ is the Kondo coupling, $\mathbf{S}^K_{\mathbf{r}}$ is the $S = 1/2$ spin operator of a magnetic atom at site $\mathbf{r}$ and $\boldsymbol{\sigma}$ are the Pauli matrices. $I_{\mathbf{r},\mathbf{r}'}$ is the antiferromagnetic coupling between magnetic atoms. In the *large-N* approach [14, 15], one represents $\mathbf{S}^K_{\mathbf{r}}$ by pseudo-fermion operators, $f^\dagger, f$, and decouples the Hamiltonian via the mean fields [16–18]

$$s(\mathbf{r}) = \frac{J}{2} \sum_\alpha \langle f^\dagger_{\mathbf{r},\alpha} c_{\mathbf{r},\alpha} \rangle; \quad \chi(\mathbf{r},\mathbf{r}') = \frac{I_{\mathbf{r},\mathbf{r}'}}{2} \sum_\alpha \langle f^\dagger_{\mathbf{r},\alpha} f_{\mathbf{r}',\alpha} \rangle. \tag{2}$$

A non-zero hybridization $s(\mathbf{r})$ between the c- and f-electron states describes the screening of a magnetic moment, and the bond variable $\chi(\mathbf{r},\mathbf{r}')$ represents the antiferromagnetic (spin-liquid) correlations [12] between nearest-neighbor moments. For a translationally invariant system, $s(\mathbf{r}) = s$, $\chi(\mathbf{r},\mathbf{r}') = \chi_0$ and χ_1 for nearest and next-nearest-neighbor sites, respectively. Adding the term $\sum_{\mathbf{r},\alpha} \varepsilon_f f^\dagger_{\mathbf{r},\alpha} f_{\mathbf{r},\alpha}$ to the Hamiltonian [16–18] allows one to fix the f-electron occupancy, $\langle \hat{n}_f \rangle$, by adjusting the on-site energy ε_f. To solve the self-consistency equations, Eq.(2), for finite lifetimes of the f- and c-electron states, we rewrite them in the form

$$\begin{aligned} s(\mathbf{r}) &= -\frac{J}{\pi} \int_{-\infty}^{\infty} d\omega \; n_F(\omega) \; \mathrm{Im} G_{fc}(\mathbf{r},\mathbf{r},\omega) \; ; \\ \chi(\mathbf{r},\mathbf{r}') &= -\frac{I_{\mathbf{r},\mathbf{r}'}}{\pi} \int_{-\infty}^{\infty} d\omega \; n_F(\omega) \; \mathrm{Im} G_{ff}(\mathbf{r},\mathbf{r}',\omega) \; , \end{aligned} \tag{3}$$

where $G_{\gamma\zeta}(\mathbf{r}',\mathbf{r},\tau) = -\langle T_\tau \gamma_{\mathbf{r}'}(\tau) \zeta^\dagger_{\mathbf{r}}(0) \rangle$ ($\gamma, \zeta = c, f$, spin indices are omitted) are the full Green's function describ-

ing the hybridization of the c- and f-electron bands, with

$$\begin{aligned} G_{ff}(\mathbf{k},\omega) &= \left[(G^0_{ff}(\mathbf{k},\omega))^{-1} - s^2 G^0_{cc}(\mathbf{k},\omega)\right]^{-1} ; \\ G_{cc}(\mathbf{k},\omega) &= \left[(G^0_{cc}(\mathbf{k},\omega))^{-1} - s^2 G^0_{ff}(\mathbf{k},\omega)\right]^{-1} ; \\ G_{cf}(\mathbf{k},\omega) &= G^0_{cc}(\mathbf{k},\omega) s G_{ff}(\mathbf{k},\omega) , \end{aligned} \tag{4}$$

where $G^0_{ff} = (\omega + i\Gamma_f - \chi_{\mathbf{k}})^{-1}$, $G^0_{cc} = (\omega + i\Gamma_c - \varepsilon_{\mathbf{k}})^{-1}$, and Γ_c^{-1} and Γ_f^{-1} are the lifetimes of the c- and f-electron states, respectively. For $\Gamma_c = \Gamma_f = 0^+$, the poles of the above Green's functions yield two energy bands

$$E^{\pm}_{\mathbf{k}} = \frac{\varepsilon_{\mathbf{k}} + \chi_{\mathbf{k}}}{2} \pm \sqrt{\left(\frac{\varepsilon_{\mathbf{k}} - \chi_{\mathbf{k}}}{2}\right)^2 + s^2} \tag{5}$$

with $\chi_{\mathbf{k}} = -2\chi_0(\cos k_x + \cos k_y) - 4\chi_1 \cos k_x \cos k_y + \varepsilon_f$.

To compute the differential conductance, dI/dV [19–21], measured in STS experiments [8, 9], we define the spinor $\Psi^\dagger_{\mathbf{k}} = (c^\dagger_{\mathbf{k}}, f^\dagger_{\mathbf{k}})$ and the Green's function matrix $\hat{G}(\mathbf{k},\tau) = -\langle T_\tau \Psi_{\mathbf{k}}(\tau)\Psi^\dagger_{\mathbf{k}}(0)\rangle$. With t_c and t_f being the tunneling amplitudes into the c- and f-electron bands, respectively, one has in the weak-tunneling limit [20]

$$\frac{dI(\mathbf{r},\omega)}{dV} = -\frac{2e}{\hbar}\hat{N}_t \sum_{i,j=1}^{2} \left[\hat{t}\,\mathrm{Im}\hat{G}(\mathbf{r},\mathbf{r},\omega)\,\hat{t}\right]_{ij} \tag{6}$$

where $\hat{t} = \begin{pmatrix} t_c & 0 \\ 0 & t_f \end{pmatrix}$, and N_t is the STS tip's density of states. To gain insight into the momentum resolved electronic structure of URu_2Si_2, Schmidt *et al.* [8] performed a quasi-particle interference (QPI) analysis via the substitution of U by Th atoms. The measured QPI intensity, $S(\mathbf{q},\omega)$, is given by the Fourier transform of dI/dV into $\mathbf{q}$-space, yielding

$$\begin{aligned} S(\mathbf{q},\omega) &\equiv \frac{dI(\mathbf{q},\omega)}{dV} = \frac{2\pi e}{\hbar} N_t \sum_{i,j=1}^{2} \left[\hat{t}\hat{N}(\mathbf{q},\omega)\hat{t}\right]_{ij} ; \\ \hat{N}(\mathbf{q},\omega) &= -\frac{1}{\pi}\,\mathrm{Im}\int \frac{d^2k}{(2\pi)^2}\hat{G}(\mathbf{k},\omega)\hat{U}\hat{G}(\mathbf{k}+\mathbf{q},\omega) . \end{aligned} \tag{7}$$

$\hat{U} = \begin{pmatrix} U_c & 0 \\ 0 & U_f \end{pmatrix}$ and U_c and U_f are the Th atoms' scattering potential in the c- and f-electron bands, respectively.

We begin by discussing the STS results of Schmidt *et al.* [8] and present in Fig. 1(a) the experimentally measured change in dI/dV below the HOT [$T = 1.9$K data of Fig. 3(b) in Ref. [8]] together with a theoretical fit, $\delta(dI/dV) = dI/dV(T < T_0) - dI/dV(T = T_0)$ (with $s = 0$ at $T = T_0$) obtained from Eq.(6). For the same parameter set as in Fig. 1(a), we present in Figs. 1(c) and (e) [(d) and (f)] a contour plot of the QPI intensity, $|S(\mathbf{q},\omega)|$, and the maxima in $|S(\mathbf{q},\omega)|$ (i.e., the QPI dispersion), respectively, along $q_y = 0$ [$q_y = q_x$]. Also shown are the experimental QPI dispersions (black lines) of Figs. 5(c)

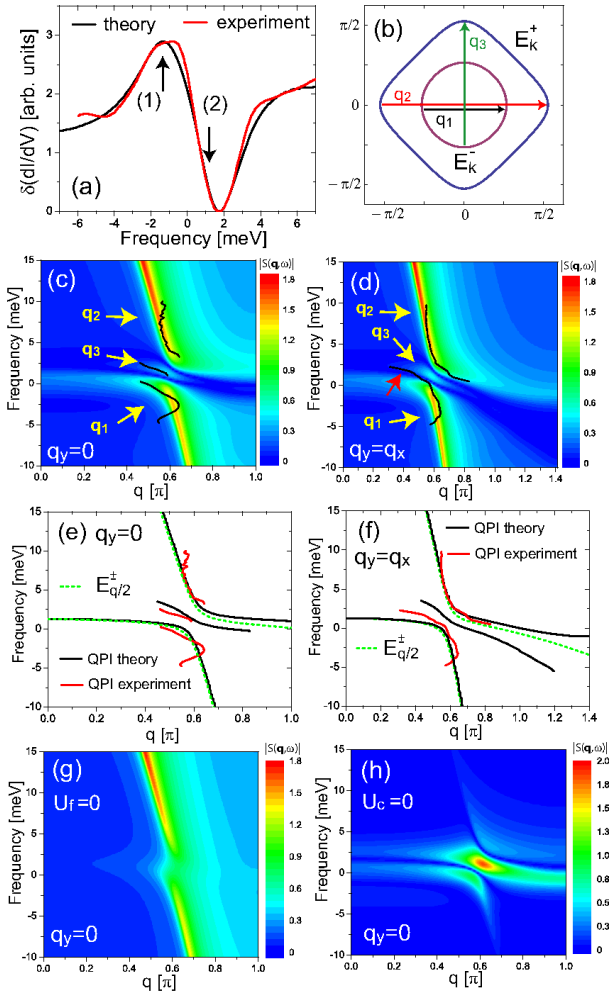

FIG. 1: (color online) (a) Experimental [8] and theoretical $\delta(dI/dV)$ below the HOT. A background was subtracted and the data were vertically scaled. (b) Fermi surfaces of $E^{\pm}_{\mathbf{k}}$. Contour plot of $|S(\mathbf{q},\omega)|$ along (c) $q_y = 0$ and (d) $q_y = q_x$, together with the QPI dispersions of Ref. [8]. $|S(\mathbf{q},\omega)|$ along $q_y = 0$ for (e) $U_f = 0$ and (f) $U_c = 0$. The theoretical results were obtained with $t = 45$ meV, $\mu = 3.17t$, $s = 0.06t$, $\varepsilon_f = -0.08t$, $\chi_0 = -0.04t$, $\chi_1 = -0.3\chi_0$, $\Gamma_{f,c} = 0.03t$, $t_f/t_c = 0.0075$, $U_f/U_c = 0.6$, yielding $J = 2.95t$, $I = 0.42t$, $n_f = 1.52$.

and (d) in Ref. [8]. The experimental dI/dV and QPI data were obtained on a U-terminated surface of a 1% Th-doped sample. The very good quantitative agreement between the theoretical and experimental dI/dV and QPI dispersions (arising from a unique set of parameters) strongly suggests that their origin lies in the emergence of a coherent Kondo lattice below the HOT, in agreement with the conclusions by Schmidt *et al.* [8] (similar STS signatures of a coherent Kondo lattice were recently also reported in $YbRh_2Si_2$ [22]).

The QPI pattern is determined by scattering of electrons both within and between the two electronic bands, $E^{\pm}_{\mathbf{k}}$. Intraband scattering [see Fig. 1(b)] gives rise to the $\mathbf{q}_1$ and $\mathbf{q}_2$ branches in $|S(\mathbf{q},\omega)|$ shown in Figs. 1(c) and

(d). The main contribution to these branches arises from $2k_F$-scattering [Fig. 1(b)], such that their dispersion is approximately described by $E^{\pm}_{\mathbf{q/2}}$ as shown in Figs. 1(e) and (f). Moreover, for -1 meV $\lesssim \omega \lesssim 1.5$ meV, $E^{\pm}_{\mathbf{k}}$ both possess equal energy surfaces, giving rise to interband scattering with wave-vector $\mathbf{q}_3$, and a corresponding $\mathbf{q}_3$ branch in $|S(\mathbf{q},\omega)|$ [see Figs. 1(c) and (d)]. The $\mathbf{q}_3$ branch has also been seen experimentally along $q_y = 0$, where the experimental and theoretical QPI results are in very good agreement, but is absent along $q_y = q_x$. The latter could arise from the smaller gap along $q_y = q_x$ which might make it difficult to resolve the $\mathbf{q}_1$ and $\mathbf{q}_3$ branches. Additional support for this conclusion comes the experimental dI/dV data in Fig. 1(a). Here, the upper band edge of $E^{-}_{\mathbf{k}}$ leads to a sharp decrease in dI/dV [see arrow (2)] which occurs around $\omega \approx 1$ meV. This energy is consistent with the extrapolation of the experimental $\mathbf{q}_1$ dispersion along $q_y = 0$ [Fig. 1(c)], where the $\mathbf{q}_1$ and $\mathbf{q}_3$ branches are well resolved, but inconsistent with the extrapolation along $q_y = q_x$. Note that the peak in dI/dV at $\omega = -2$ meV [see arrow (1) in Fig. 1(a)] arises from the van Hove singularity of the f-electron band.

The experimental QPI pattern implies that the doped Th atoms scatter electrons in both the c- and f-electron bands [8]. To support this conclusion, we present in Fig. 1(g) the QPI pattern, $|S(\mathbf{q},\omega)|$, for $U_f = 0$. It is similar to that of the unhybridized c-electron band [see Fig. 3(a)] since its dominant contribution arises from scattering between states where the coherence factors of the c-electrons are large. Conversely, for $U_c = 0$, [Fig. 1(h)], $|S(\mathbf{q},\omega)|$ is determined by scattering between states with large f-electron weight. Both cases are inconsistent with the experimental QPI results, whose description requires $U_f/U_c \approx 0.6$, as shown in Fig. 1.

We next discuss the STS results by Aynajian *et al.* [9], and present in Figs. 2(a) and (b) the experimental dI/dV data obtained on a U-terminated surface of pure URu_2Si_2 for $T = 2$K and 4K, respectively [Fig. 4(b) in Ref. [9]], together with the theoretical results obtained from Eq.(6). The theoretical dI/dV curves reproduce the salient features of the experimental results: the asymmetry and magnitude of the gap in dI/dV as well as the peak at $\omega \approx -0.8$ meV [see arrows in Figs. 2(a) and (b)] which arises from the van Hove singularity of the f-electron band (a similar peak and gap magnitude were also reported for a Si-terminated surface in Ref.[8]). Both, the gap asymmetry and the peak, are characteristic signatures of the Kondo lattice bandstructure, and thus suggest the existence of a coherent Kondo lattice below the HOT. To gain further insight into the microscopic origin of the CKL, we note that the changes in dI/dV between $T = 2$K [Fig. 2(a)] and $T = 4$K [Fig. 2(b)] can be solely attributed to an increase in the damping of the f-electron states from $\Gamma_f = 0.013t$ at $T = 2$K to $\Gamma_f = 0.02t$ at $T = 4$K, and the resulting changes in s, χ_0

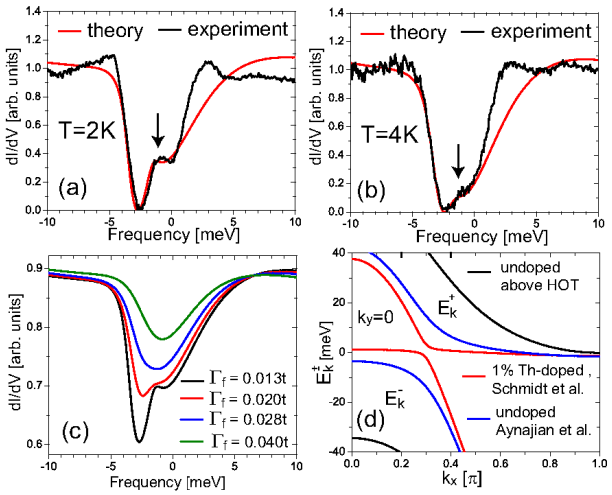

FIG. 2: (color online) Theoretical fits to the dI/dV data of Ref. [9] at (a) $T = 2$K and (b) $T = 4$K. (c) Evolution of dI/dV with Γ_f. The theoretical results were obtained with $J = 3.69t$, $I = 0.89t$, $n_f = 1.59$, $\chi_1 = -0.36\chi_0$, $t_f/t_c = 0.0175$, and $\Gamma_c = 0.02t$. At $T = 2$K, $s = 0.32t$, $\varepsilon_f = -0.20t$, $\chi_0 = -0.09t$. (d) $E^{\pm}_{\mathbf{k}}$ extracted from theoretical fits.

and ε_f which are self-consistently computed from Eq.(3) for fixed J, I and n_f. Increasing Γ_f even further (while self-consistently computing s, χ_0 and ε_f) yields the evolution of dI/dV shown in Fig. 2(c) which possesses the same characteristic signatures as those observed by Aynajian *et al.* [9] with increasing temperature. In particular, the gap in dI/dV is filled in, its magnitude remains approximately constant (until close to the HOT), and the center of the gap shifts to larger energies with increasing temperature or Γ_f. Both s and χ_0 decrease with increasing Γ_f (not shown) since the increased decoherence of the f-electron states necessarily suppresses coherent Kondo screening and magnetic correlations. The results in Figs. 2(a)-(c) suggest that the formation of a coherent Kondo lattice below the HOT is driven by a drastic increase in the f-electron lifetime. In contrast, increasing solely the hybridization, s, below the HOT leads to an evolution of dI/dV (not shown) that is inconsistent with the experimental observations.

In Fig.2(d), we present the bandstructure, $E^{\pm}_{\mathbf{k}}$, obtained from the fits to the STS data by Schmidt *et al.* for the 1% Th-doped sample [Fig. 1] and by Aynajian *et al.* [9] for pure URu_2Si_2 [Fig.2(a)]. In the Th-doped sample, the hybridization ($s = 0.06t$) is smaller while $\Gamma_{f,c}$ are larger than in the undoped compound ($s = 0.32t$). These results are consistent with a suppression of the HOT (and thus s) and an increased decoherence by Th-doping, and thus suggest that both groups probe the same heavy and light bands (while irrelevant for our study, we note that the groups disagree on the identification of the cleaved surfaces). Further support for this conclusion comes from the extracted f-electron density, which is quite similar in

both cases with $n_f = 1.59$ in the pure and $n_f = 1.52$ in the Th-doped sample. While these values deviate from the constraint $n_f = 1$ usually enforced in the Kondo limit [14], the good agreement between the theoretical and experimental results suggest that corrections due to valence fluctuations are small.

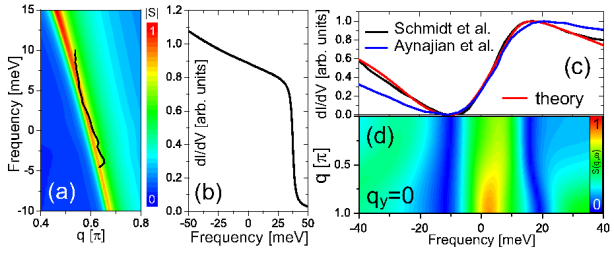

FIG. 3: (color online) (a) $|S(\mathbf{q},\omega)|$ for $q_x = q_y$ together with the experimental QPI dispersion of Ref. [8], and (b) dI/dV, both for the same parameters as in Fig. 1 but $s = 0$. (c) Theoretical fit to the 19K dI/dV data [Fig.5(c) in Ref. [8]] with $s = 1.0t$, $\chi_0 = -0.045t$, $\chi_1 = 0$, $\varepsilon_f = -0.032t$, $\Gamma_c = 0.77t$, $\Gamma_f = 0.13t$, and (d) the resulting $|S(\mathbf{q},\omega)|$ along $q_y = 0$.

Finally, we discuss the dI/dV Fano-lineshape observed above the HOT [8, 9] and its relation to the conduction band observed in QPI [8]. To this end, we extend our analysis of the STS results by Schmidt *et al.*[8] by assuming a vanishing hybridization, $s = 0$, for $T > T_0$. The resulting QPI intensity $|S(\mathbf{q},\omega)|$ shown in Fig. 3(a) reproduces well the experimental QPI dispersion (black line) of Fig. 5(b) in Ref. [8]. Due to the smallness of $t_f/t_c = 0.0075$, and since $s = 0$, the contribution of the heavy f-electron band to $|S(\mathbf{q},\omega)|$ and dI/dV is negligible, thus explaining its absence in the experimental QPI data above the HOT [8]. However, the resulting dI/dV lineshape does not exhibit the characteristic Fano form, implying that its origin resides in electronic bands not yet seen in QPI (the sharp drop in dI/dV at $\omega \approx 40$meV signifies the upper band edge of $\varepsilon_{\mathbf{k}}$). To further investigate this possibility, we present in Fig. 3(c) a theoretical fit using Eq.(6) to the experimental dI/dV data of Ref. [8] above the HOT on a Si-terminated surface in a pure sample, which are similar to those of Ref. [9] on a U-terminated surface. The resulting bands, $E^{\pm}_{\mathbf{k}}$, shown in Fig. 2(d), are not only significantly different from the ones seen in QPI below the HOT, but also exhibit much larger quasi-particle dampings, $\Gamma_{f,c}$, thus representing an *incoherent Kondo lattice*. As a result, $|S(\mathbf{q},\omega)|$, shown in Fig. 3(d), exhibits very little $\mathbf{q}$-structure (for fixed ω), thus explaining the difficulty in detecting these bands in QPI. We therefore conclude that an explanation of the STS data above and below the HOT requires multiple sets of c- and f-electron bands.

We have shown that the STS results by Schmidt *et al.* [8] and Aynajian *et al.* [9] are consistent with the emergence of a coherent Kondo lattice below the HOT in URu_2Si_2. While it is not expected that the CKL is the primary origin of the HOT [15], it could be a result of the HOT. In particular, one might speculate that the emergence of a yet unknown order parameter at T_0 could lead to a significant decrease in the quasi-particle decoherence, for example, through the gapping of low-energy excitations, and thus induce the formation of a coherent Kondo lattice, as described above. Clearly, further studies are required to investigate this possibility.

We would like to thank P. Aynajian, J.C. Davis, and A. Yazdani for stimulating discussions and comments, and for providing us with their experimental data. This work is supported by the U.S. Department of Energy under Award No. DE-FG02-05ER46225.

[1] M.B. Maple *et al.*, J. Low Temp. Phys. **99**, 223 (1995); A. Schroder *et al.* Nature (London) **407**, 351 (2000); G.R. Stewart, Rev. Mod. Phys. **73**, 797 (2001); J. Custers, *et al.* Nature (London) **424**, 524 (2003); H. von Lohneysen *et al.*, Rev. Mod. Phys. **79**, 1015 (2007); P. Gegenwart, Q. Si, and F. Steglich, Nature Physics, **4**, 186 (2008).
[2] J. Kondo, Prog. Theor. Phys. **32**, 37 (1964).
[3] S. Doniach, Physica B **91**, 231 (1977).
[4] T. T. M. Palstra *et al.* Phys. Rev. Lett. **55** 2727 (1985).
[5] M.B. Maple, *et al.* Phys. Rev. Lett. **56**, 185 (1986).
[6] J. Schoenes *et al.*, Phys. Rev. B **35**, 5375 (1987); D.A. Bonn *et al.*, Phys. Rev. Lett. **61**, 1305 (1988); S.V. Dordevic, *et al.*, Phys. Rev. Lett. **86**, 684 (2001); J.G. Rodrigo *et al.* Phys. Rev. B. **55**, 14318 (1997); R. Escudero, F. Morales, and P. Lejay, Phys. Rev. B **49**, 15271 (1994); J.D. Denlinger *et al.*, J. Elec. Spectrosc. **117?118**, 347 (2001).
[7] D.L. Cox, Phys Rev Lett **59**, 1240 (1987); P. Chandra *et al.*, Nature **417**, 831 (2002); C.M. Varma and L. Zhu, Phys. Rev. Lett. **96**, 036405 (2006); K. Haule, and G. Kotliar, Nature Phys. **5**, 796 (2009); A.V. Balatsky *et al.*, Phys. Rev. B **79**, 214413 (2009); S. Elgazzar, *et al.*, Nature Mater. **8**, 337 (2009); P. M. Oppeneer *et al.*, Phys. Rev. B **82**, 205103 (2010); C. Pepin *et al.*, arXiv:1010.1237; Y. Dubi and A.V. Balatsky, arXiv:1011.5315.
[8] A.R. Schmidt *et al. Nature* **465**, 570 (2010).
[9] P. Aynajian *et al.*, PNAS **107**, 10383 (2010).
[10] U. Fano, Phys. Rev. **124**, 1866 (1961).
[11] Q.M. Si *et al.*, Nature **413**, 804 (2001).
[12] T. Senthil, S. Sachdev, and M. Vojta, Phys. Rev. Lett. **90**, 216403 (2003); I. Paul, C. Pepin, and M.R. Norman, Phys. Rev. Lett. **98**, 026402 (2007).
[13] P. Coleman, *Handbook of Magnetism and Advanced Magnetic Materials* (Wiley and Sons, 2007).
[14] N. Read and D. M. Newns, J. Phys. C **16**, 3273 (1983); P. Coleman, Phys. Rev. B **28**, 5255 (1983); N. E. Bickers, Rev. Mod. Phys. **59**, 845 (1987); A.J. Millis and P.A. Lee, Phys. Rev. B **35**, 3394 (1987).
[15] A. D. Hewson, *The Kondo Problem to Heavy Fermions* (Cambridge University Press, Cambridge, 1997).
[16] J.R. Iglesias, C. Lacroix, and B. Coqblin, Phys. Rev. B **56**, 11820 (1997).
[17] R.K. Kaul and M. Vojta, Phys. Rev. B **75**, 132407 (2007).
[18] J.Figgins and D.K. Morr, preprint, arXiv:1001.3875.

[19] M. Maltseva, M. Dzero, and P. Coleman, Phys. Rev. Lett. **103**, 206402 (2009).
[20] J. Figgins, and D.K. Morr, Phys. Rev. Lett. **104**, 187202 (2010).
[21] P. Wölfle, Y. Dubi, and A.V. Balatsky, Phys. Rev. Lett. **105**, 246401 (2010).
[22] S. Ernst *et al.*, preprint.